J Comp Physiol B (2008) 178:285–295
DOI 10.1007/s00360-007-0221-0

ORIGINAL PAPER

Molecular identification, immunolocalization, and functional activity of a vacuolar-type H^+-ATPase in bovine rumen epithelium

Elke Albrecht · Martin Kolisek · Torsten Viergutz · Rudolf Zitnan · Monika Schweigel

Received: 9 July 2007 / Revised: 12 October 2007 / Accepted: 22 October 2007 / Published online: 8 November 2007
© Springer-Verlag 2007

Abstract In this study, we have studied the expression, localization, and functionality of vacuolar-type H^+-ATPase (vH^+-ATPase) and Na^+/K^+-ATPase in the bovine rumen epithelium. Compared with the intracellular pH (pH_i) of control rumen epithelial cells (REC; 7.06 ± 0.07), application of inhibitors selective for vH^+-ATPase (foliomycin) and Na^+/K^+-ATPase (ouabain) reduced pH_i by 0.10 ± 0.03 and 0.18 ± 0.03 pH-units, respectively, thereby verifying the existence of both functional proteins. Results from qRT-PCR and immunoblotting clearly confirm the expression of vH^+-ATPase B subunit in REC. However, the amount of Na^+/K^+-ATPase mRNA and protein is ten-fold and 11-fold of those of vH^+-ATPase subunit B, respectively, reflecting a lower overall abundance of the latter in REC. Na^+/K^+-ATPase immunostaining has revealed the protein in the plasma membrane of all REC from the stratum basale to stratum granulosum, with the highest abundance in basal cells. In contrast, the vH^+-ATPase B subunit has been detected in groups of cells only, mainly localized in the stratum spinosum and stratum granulosum of the epithelium. Furthermore, vH^+-ATPase has been detected in the cell membrane and in intracellular pools. Thus, functional vacuolar-type H^+ pumps are expressed in REC and probably play a role in the adaptation of epithelial transport processes.

Keywords Rumen epithelial cells · Immunohistochemistry · Proton pump · Na^+/K^+-ATPase · BCECF

Communicated by G. Heldmaier.

E. Albrecht
Muscle Biology and Growth, Research Institute for the Biology of Farm Animals (FBN), Wilhelm-Stahl-Allee 2, 18196 Dummerstorf, Germany

M. Kolisek
Department of Veterinary Physiology, Faculty of Veterinary Medicine, Free University of Berlin, Oertzenweg 19b, 14163 Berlin, Germany

T. Viergutz
Reproductive Biology, Research Institute for the Biology of Farm Animals (FBN), Wilhelm-Stahl-Allee 2, 18196 Dummerstorf, Germany

R. Zitnan
Research Institute of Animal Production, Slovak Agricultural Research Centre, Nitra, Komenskeho 73, 041 81 Kosice, Slovakia

M. Schweigel
Research Institute for the Biology of Farm Animals (FBN), Wilhelm-Stahl-Allee 2, 18196 Dummerstorf, Germany

M. Schweigel (✉)
Department of Nutritional Physiology "Oskar Kellner", Research Institute for the Biology of Farm Animals (FBN), Wilhelm-Stahl-Allee 2, 18196 Dummerstorf, Germany
e-mail: mschweigel@fbn-dummerstorf.de

Abbreviations

REC	Rumen epithelial cells
vH^+-ATPase	Vacuolar-type H^+-ATPase
pH_i	Intracellular pH

Introduction

The multilayer rumen epithelium not only has protective functions but also play a considerable role in the absorption of nutrients, mainly of short chain fatty acids (SCFA) and of electrolytes (Sehested et al. 1996, 1999). Active transport proteins, ATPases, are key transport elements required

for the establishment of electrochemical gradients driving cellular transport processes and directed substrate flow across epithelia (Ehrenfeld and Klein 1997; Zouzoulas et al. 2005). Moreover, they are also involved in the processes such as cell maintenance and proliferation (Karwatowska-Prokopczuk et al. 1998; Rozengurt 1980; Sennoune et al. 2004; Standley et al. 1997). However, our knowledge of active transport mechanisms in rumen epithelium is limited. A Na^+/K^+-ATPase has been shown to be expressed at high levels (Hansen 1998; Kristensen et al. 1995) and to account for approximately 22–25% of the rumen utilization of O_2 and, consequently, of ATP (Kelly et al. 1993). Hansen (1998) has identified the catalytic subunit of the rumen epithelium Na^+/K^+-ATPase as being the α_1-isoform. By using immunohistochemistry, Graham and Simmons (2005) have directly shown the localization of the Na^+/K^+-ATPase in the plasma membrane, with a concentration of the pump in cells of the stratum basale and decreasing density toward the lumen. However, only recently, we have found molecular evidence for the expression of a second active transport mechanism, namely a vacuolar-type H^+-adenosine triphosphatase (vH^+-ATPase) in cultured sheep rumen epithelial cells (REC) (Etschmann et al. 2006); we have demonstrated the functional activity of the vH^+-ATPase by establishing that it contributes considerably to H^+ secretion and therefore plays an important role in the regulation of the internal pH (pH_i) of REC. The application of foliomycin, a well-known high-specific vH^+-ATPase inhibitor (Drose et al. 1993), leads to a fast reduction of the pH_i. Moreover, in a former study (Schweigel and Martens 2003), we have observed that the Mg^{2+} influx and thereby the free intracellular $[Mg^{2+}]_i$ is reduced in REC treated with vH^+-ATPase inhibitor. A link between electrogenic H^+ secretion by vH^+-ATPases localized on the cell membrane and ion transport and/or the regulation of cytosolic pH has also been found in other epithelia, e.g., frog skin, mammalian renal collecting duct, and epididymis (Brown and Breton 1996; Ehrenfeld and Klein 1997; Gluck et al. 1992). In monolayer epithelia of kidney (proximal and distal convoluted tubules, thick ascending limbs of Henle, α-intercalated cells of the collecting duct), epididymis and vas deference, the vH^+-ATPase is mainly localized in the apical membrane (Brown and Breton 2000; Pastor-Soler et al. 2003).

To date, no information is available concerning the existence or cellular and subcellular distribution of vH^+-ATPase in bovine rumen epithelium. Therefore, the main objective of the current study has been a comparative investigation of Na^+/K^+-ATPase and vH^+-ATPase expression and the localization in this tissue by quantitative reverse transcription-polymerase chain reaction (qRT-PCR), Western blotting, and immunohistochemistry. The functional activity of these transport proteins has also been investigated by measurements of pH_i by using the membrane-permeable fluorescent probe 2′,7′-bis(2-carboxyethyl)-5(6)-carboxyfluorescein acetoxymethyl ester (BCECF-AM) and the application of respective transport inhibitors (ouabain and foliomycin) to differentiate between Na^+/K^+-ATPase and vH^+-ATPase activity.

As expected, we have found highly abundant Na^+/K^+ pumps in the cell membrane of all REC, with the exception of those in the stratum corneum. In addition, we have shown the expression of functional vH^+-ATPases localized in cell membranes and/or cytosolic pools of the more luminally oriented cell layers (stratum spinosum and stratum granulosum) of the rumen epithelium.

Materials and methods

Materials

Medium 199, trypsin, glutamine, penicillin-streptomycin, Dulbecco's phosphate-buffered saline (DPBS), and fetal calf serum (FCS) were purchased from PAN Biotech (Aidenbach, Germany). BCECF-AM, pluronic acid, and propidium iodide were from Molecular Probes Inc. (Eugene, OR). Foliomycin was from ICN (Aurora, Ohio) and ouabain from Sigma. RT-PCR and qRT-PCR reagents were purchased from Biorad (Hercules, CA). All other chemicals (TritonX-100, PBS) were obtained from Sigma.

Antibodies

The monoclonal mouse antibodies used in this study were specific for 60-kDa subunit of the yeast vH^+-ATPase (13D11-B2, Molecular Probes) and the α subunit of the sheep Na^+/K^+-ATPase (M7-PB-E9, Affinity Bioreagents). Additionally, a polyclonal goat anti-vH^+-ATPase human B1/2 subunit antibody (L 20, Santa Cruz) was used in some of the immunohistochemistry experiments. A specific monoclonal mouse antibody (B2901, Sigma) was used to detect bovine serum albumin. The relevant secondary antibodies conjugated to Alexa fluor 488 (Molecular Probes) were used for immunohistochemistry. For Western blotting, horseradish-peroxidase (HRP)-conjugated antibodies obtained from Invitrogen were used.

Animals, tissue preparation, and cell isolation

The rumenal tissues were obtained from a local slaughter house. Samples were excised from the forestomachs of cattle or sheep within 10 min of slaughter. Two pieces of rumen tissue, each about 100 cm^2, were taken from the

ventral sac, washed at least three times in ice-cold phosphate-buffered saline (PBS) containing penicillin–streptomycin, and then transported to the laboratory in the same solution. There, rumen papillae were removed by scissors and washed three times in antibiotic-containing PBS. Subsequently, REC were isolated by fractional trypsinization as described by Galfi et al. (1980). Fractions were evaluated by light microscopy and those containing mostly cells of the stratum spinosum and stratum granulosum were used in functional experiments, to prepare protein extracts, and to isolate total RNA.

Detection of specific mRNA concentration

Total RNA was isolated by a standard procedure (Invitek kit and manufacturer's protocol). The reverse transcription (RT) reaction was performed by means of an iScript cDNA synthesis kit (BioRad) with 100 ng total RNA and an oligo $(dT)_{12}$ primer to synthesize cDNA from poly-A-containing mRNA. The cDNA was amplified by real time polymerase chain reaction (PCR) (iCycler, BioRad) in an iQ-SYBR green supermix by analogy with described methods (Löhrke et al. 2005; Ulbrich et al. 2006). A 1-µl aliquot of each RT reaction (1/20 of total) was primed, in each 10 µl PCR, with gene-specific oligonucleotides (Table 1). The primers of vH^+-ATPase, Na^+/K^+-ATPase, and S18 (a ribosomal protein used as a housekeeping transcript, Ulbrich et al. 2006) were designed to span a corresponding intron and to anneal at 60°C to the published cDNA and gene sequences; the mRNA fragments produced are shown in Table 1. The specificity of the products was assessed by melting point analysis and agarose gel electrophoresis in comparison with an oligonucleotide molecular mass ladder to confirm that the calculated molecular mass of the cDNA corresponded to the produced cDNA. The cDNA structure was checked by sequencing. The mRNA abundance was calculated by using the known concentration of standard oligonucleotides and the amplification efficiency displayed by the iCycler as described elsewhere (Löhrke et al. 2005; Ulbrich et al. 2006). Results were determined as the relative expression levels of vH^+-ATPase subunit B in comparison with the relative expression level of Na^+/K^+-ATPase in REC.

Western blot analysis

For Western blots, total protein from washed REC was extracted by use of the M-PER Mammalien Protein Extraction Reagent (Pierce), complemented with a protease inhibitor cocktail (Pierce). The protein concentration was determined by using the Bradford assay (Biorad). Protein samples (40–80 µg) were separated by SDS (10%)-polyacrylamide gel electrophoresis and subsequently transferred to polyvinylidene fluoride (PVDF) membrane. After transfer, membranes were blocked with 3% non-fat dry milk in TRIS-buffered saline (pH 7.5) containing 0.05% Tween 20 (TBS-T) for 1 h. Following blocking, filters were incubated at 4°C with the primary antibodies (anti-vH^+-ATPase: 1:5,000 dilution; anti Na^+/K^+-ATPase: 1:1,000 dilution; anti bovine serum albumin: 1:2,000 dilution) overnight, washed three times for 10 min in TBS-T, and incubated for 1 h with HRP-conjugated secondary antibody (1:10,000 dilution). After incubation with the secondary antibody, filters were washed three times for 10 min in TBS-T. Bands were visualized in ChemilmagerTM 5500 (Alpha Innotech) by use of Rotilumin (Roth). Western blot images ($n = 3$) were used for digital densitometry analysis performed by E.A.S.Y Win32 software (Herolab GmbH, Germany). Digital densities (dd) of bands corresponding to vH^+-ATPase and Na^+/K^+-ATPase, respectively, were related to dd of bands corresponding to bovine serum albumin (3 µg) used as standard (st). Differences between dd of vH^+-ATPase and dd of Na^+/K^+-ATPase bands were then calculated by use of the following equation:

$$\mathrm{dd} = [\mathrm{dd}(Na^+/K^+ - \mathrm{ATPase}) : \mathrm{dd}(\mathrm{st})] / [\mathrm{dd}(vH^+ - \mathrm{ATPase}) : \mathrm{dd}(\mathrm{st})].$$

Table 1 Sequences of primer sets used for amplification of specific cDNA

Transcript	Forward primer 5′–3′	Reverse primer 5′–3′	Product (bp)	Acc. no.
vH^+-ATPase	139–162	320–297	182	gi 61553265
Subunit B	TTT TAT TGA ACA AGA AGC CAA TGA	GAT TCA TCA AAT TGG ACA TCT GAA		
S18	293–316	510–487	218	gi 74268022
	CTT AAA CAG ACA GAA GGA CGT GAA	CCA CAC ATT ATT TCT TCT TGG ACA		
Na^+/K^+-ATPase	2,595–2,618	2,821–2,798	227	gi 115305283
α Subunit	GAG ATT ACC CCC TTC CTG ATA TTT	TGG ATC ATA CCA ATC TGT CCA TAG		

Primers were constructed according to data from Gene Bank. Acc. No., bp, vH^+-ATPase, S18, and Na^+/K^+-ATPase denote the accession number, the number of base pairs, and the genes encoding vH^+-ATPase, ribosomal protein S18, and Na^+/K^+-ATPase, respectively

Immunohistochemistry

Rumen papillae were fixed in 4% paraformaldehyde in PBS overnight, washed in PBS, frozen in liquid nitrogen, and cryosectioned on a Leica CM3050 S (Leica, Bensheim, Germany). Sections (6 μm) were washed three times with PBS, permeabilized by incubation for 20 min in PBS containing 0.1% Triton X-100, and blocked with 10% rabbit serum in PBS + Triton X-100 for 15 min (all at room temperature). Subsequently, sections were incubated overnight at 4°C with primary antibody (diluted 1:50 with 2% serum in PBS + Triton X-100) in a humidity chamber. After being washed three times, sections were incubated for 45 min at room temperature in the dark with an appropriate secondary antibody labeled with Alexa Fluor 488 (Molecular Probes, Eugene, OR, USA), diluted 1:500 in PBS + Triton X-100. Nuclei were usually counterstained with 1 μg/ml propidium iodide in PBS. Sections were covered with MobiGLOW mounting medium (MoBiTec, Göttingen, Germany) and appropriate cover-slips. Sections incubated with serum in PBS + Triton X-100 instead of primary antibody were used as negative controls and showed no unspecific binding of secondary antibodies in rumen epithelial cells.

Immunofluorescence was detected by using a Nikon Microphot SA fluorescence microscope (Nikon Instruments Europe B.V., The Netherlands) and an image analysis system equipped with CELL^F image analysis software and a CC-12 high resolution color camera (OSIS, Münster, Germany).

Measurement of pH_i by spectrofluorometry

For the determination of pH_i, cells were loaded with 1 μM BCECF-AM for 30 min and subsequently washed twice in DPBS. Rumen epithelial cells (REC) were incubated for a further 30 min to allow complete de-esterification and washed twice before measurement of fluorescence. Intracellular pH (pH_i) was determined by measuring the fluorescence of the probe-loaded REC in a spectrofluorometer (LS-50 B, Perkin-Elmer) equipped with a fast-filter accessory that allowed fluorescence to be measured at 20-ms intervals with excitation for BCECF at 440 and 480 nm and emission at 515 nm. All measurements were made at 37°C in a 3-ml cuvette containing 2 ml cell suspension (10% cytocrit) under stirring. The HCO_3^- free, HEPES-buffered measuring solution had the following composition (in mM): 125 NaCl, 20 Na-butyrat, 5 KCl, 1 $CaCl_2$, 2 $MgCl_2$, 10 HEPES, 5 glucose, pH 7.4. This solution was selected to exclude Na^+–HCO_3^- symporter related pH_i regulation (Müller et al. 2000) and to ensure comparability of the data with results from our previous study with sheep REC (Etschmann et al. 2006). In inhibitor studies specific blockers for vH^+-ATPase (2 μM foliomycin), Na^+/K^+-ATPase (0.5 mM ouabain) and Na^+/H^+ exchanger (0.25 mM amiloride) were added to the measuring solution.

BCECF signals were calibrated to pH by placing the cells in medium containing 135 mM KCl and the ionophore nigericin (10 μM) to equilibrate intra- and extracellular $[H^+]$. The procedure was repeated for various pH values between 6.0 and 8.0. For data evaluation, 10-s data sets were each averaged at the beginning of the measurement and then after 50, 100, 150, 200, 250, 300, 350, 400, 450, 500, and 550 s. The final pH_i was determined as the mean pH_i of the last 10 s of the measurement. Thus, for the calculation of any given pH_i value, 500 data points were used.

Statistical analysis

If not otherwise stated, data are presented as means ± standard error (SE). Significance was determined by Student's *t* test or the paired *t* test as appropriate. $P < 0.05$ was considered to be significant. All statistical calculations were performed by using SigmaStat (Jandel Scientific).

Results

Expression of vH^+-ATPase subunit B and Na^+/K^+-ATPase α subunit mRNA

As shown in Fig. 1a, the products obtained by RT-PCR corresponded to the calculated base number of the sequence produced by the primers shown in Table 1. These results were confirmed by sequencing the products, yielding an identity of 99–100% homology. The steady-state concentration of vH^+-ATPase subunit B mRNA was 0.011 ± 0.001 pg per pg S18 mRNA control. The mean amount of Na^+/K^+-ATPase α subunit mRNA was 0.090 ± 0.002 pg per pg S18 mRNA control.

Immunoblot of the REC vH^+- and Na^+/K^+-ATPase

The results of Western blot analyses are shown in Fig. 1b. In immunoblots of protein lysates from REC, the anti-yeast vH^+-ATPase antibody labeled a 60-kDa protein representing subunit B of vH^+-ATPase. In addition, a 110-kDa immunoreactive band was constantly detected showing the existence of the Na^+/K^+-ATPase α subunit at the protein level. Digital density analysis ($n = 3$) with bovine serum

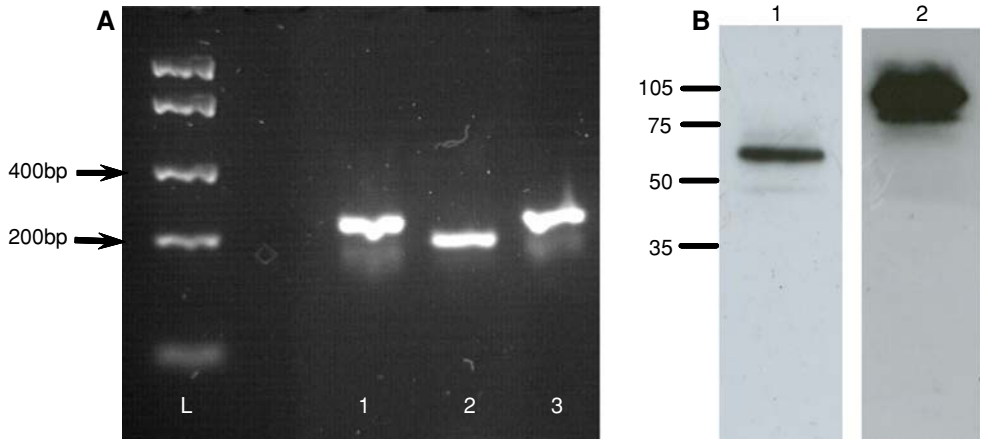

Fig. 1 Detection of mRNA and protein from vH^+-ATPase subunit B and Na^+/K^+-ATPase subunit α in bovine REC. **a** Ethidium bromide-stained agarose gel of RT-PCR products for DNA size ladder (bp, lane L), S18 (218 bp, lane 1), vH^+-ATPase subunit B (182 bp, lane 2), and Na^+/K^+-ATPase α subunit (227 bp, lane 3). **b** Immunoblot of the vH^+-ATPase B-subunit (60 kDa, lane 1) and the Na^+/K^+-ATPase α-subunit (110 kDa, lane 2). Antibodies directed against the α subunit of the sheep Na^+/K^+-ATPase and the 60-kDa subunit of the yeast vH^+-ATPase were used. Blots are representative of data from eight animals

albumin as internal standard revealed that Na^+/K^+-ATPase α subunit is 11.3 ± 0.9 times more abundant than vH^+-ATPase in the analyzed samples.

Immunolocalization of Na^+/K^+-ATPase α subunit and of vH^+-ATPase B subunit in bovine rumen epithelium

For a better understanding of the following data, the morphology of the rumen epithelium is shown in Fig. 2. As can be seen in Fig. 2a, it forms luminal extensions consisting of leaf-like papillae that extend the total surface area. Compared with the single layer of renal or intestinal epithelia, the rumen epithelium has a more complex multilayered structure. Starting from the blood side, four distinct cell layers, namely, the stratum basale, the stratum spinosum, the stratum granulosum, and the keratinized stratum corneum, can be distinguished (Fig. 2b).

The α subunit-specific anti-Na^+/K^+-ATPase antibody identified the protein in the cell membrane of REC from the stratum basale to the stratum granulosum (Fig. 3a). The Na^+/K^+-ATPase was enriched in cells of the stratum basale with the highest expression toward the basal plasma membrane of these cells. A progressive reduction of the immunostaining intensity was observed in the cells of the stratum spinosum and stratum granulosum, and no staining was seen in the stratum corneum. The cellular distribution of the Na^+/K^+-ATPase in samples from sheep rumen epithelium was identical to that observed in bovine samples (Fig. 3b).

To determine the relative cellular and subcellular distribution of the vH^+-ATPase in bovine rumen epithelium,

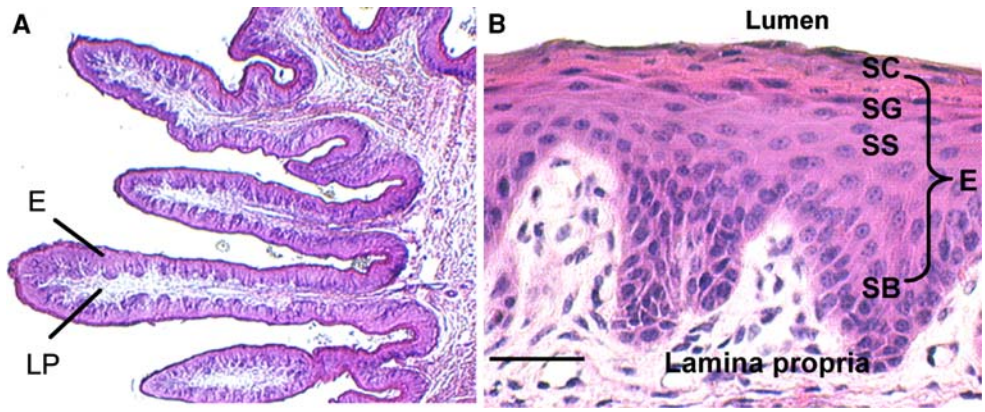

Fig. 2 Transmitted light photomicrograph of the multilayered bovine ruminal epithelium stained with hematoxylin–eosin. **a** Cross section of complete rumen papillae, *E*, stratified epithelium; *LP*, lamina propria containing vasculature and connective tissue. **b** Cross section of a single papilla, *SC*, stratum corneum; *SG*, stratum granulosum; *SS*, stratum spinosum; *SB*, stratum basale; *E*, epithelium. *Scale bar* = 50 μm

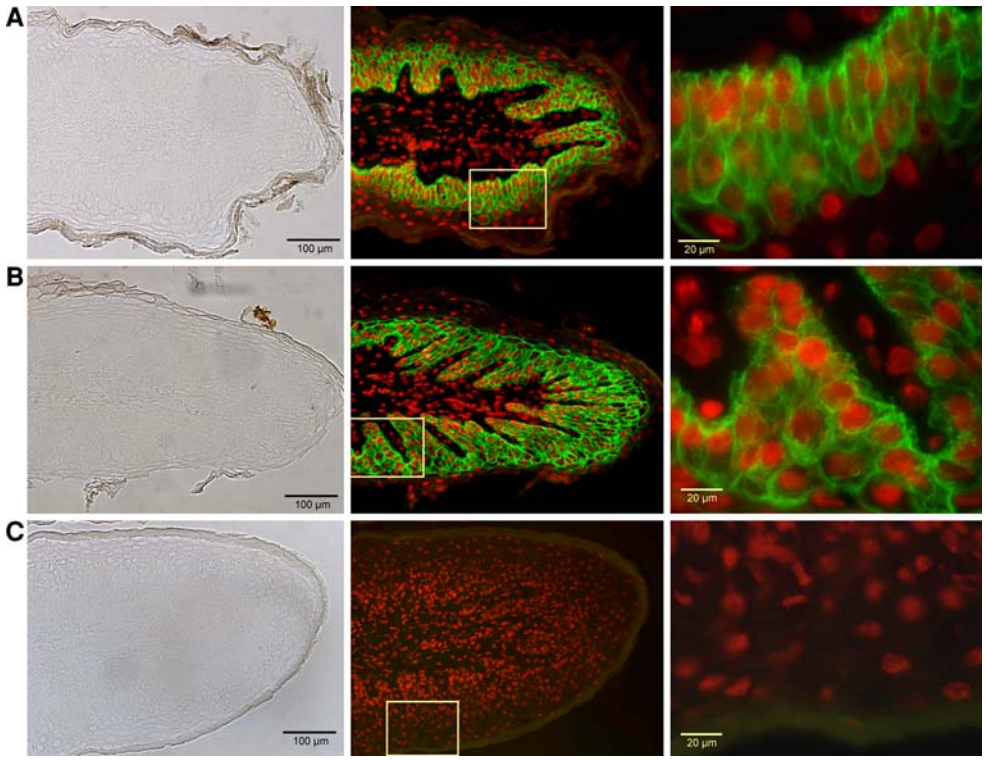

Fig. 3 Immunolocalization of Na^+/K^+-ATPase α-subunit (*light gray*) in bovine (**a**) and ovine (**b**) rumen epithelium using a monoclonal mouse antibody against sheep Na^+/K^+-ATPase and an Alexa fluor 488 conjugated secondary antibody (*left*: transmitted-light micrograph; *middle*: fluorescent image of same area; *right*: higher magnification of *boxed area*). **c** negative control: section of a rumen papilla with primary antibody omitted. Cells were co-stained with propidium iodide (*gray*) to label nuclei. Note that the Na^+/K^+-ATPase is concentrated in the basal cell layers, especially toward the basal lamina. Staining intensity decreased across the stratum spinosum to stratum granulosum

we used antibodies directed either against the 60-kDa subunit of the yeast vH^+-ATPase or the B1 and B2 subunit of the human vH^+-ATPase. Both antibodies were able to detect vH^+-ATPase in bovine rumen epithelium, but in comparison with the Na^+/K^+-ATPase, the vH^+-ATPase B subunit expression level was considerably lower (Fig. 4). Moreover, the occurrence and distribution of the protein showed a much higher variability. Examples of characteristic staining patterns are given in Fig. 4. Typically, the anti-vH^+-ATPase subunit B antibody labeled groups of cells predominantly localized in the stratum spinosum and stratum granulosum. The staining intensity was much lower or more punctuate in stratum basale cells, and no specific immunostaining appeared in the stratum corneum. The vH^+-ATPase B subunit was dominantly localized in the cell membrane or in its close vicinity (Fig. 4a), although cytoplasmic staining was also observed (Fig. 4b).

Functional activity of vH^+-ATPase and Na^+/K^+-ATPase in bovine rumen epithelium

The functional activity of both transport proteins was investigated in inhibitor studies with foliomycin and ouabain as blockers specific for vH^+-ATPase and Na^+/K^+-ATPase, respectively. BCECF-loaded REC were suspended in HEPES-buffered NaCl-medium with butyrate (20 mM) containing ouabain (0.5 mM), foliomycin (2 µM), or both inhibitors. After a 5-min pre-incubation period in this medium, the pH_i was measured continuously over a 10-min period. Control measurements were performed with cells handled in the same way, but without any blocker present in the solutions. Records from a typical experiment are shown in Fig. 5a. Under control conditions, we measured a pH_i of 7.06 ± 0.07 at the beginning and of 7.19 ± 0.06 at the end of the measuring period. In comparison with the pH_i of these control cells, inhibitor-treated REC showed a decreased pH_i (for a summary of the results under all conditions, see Fig. 5a). Five minutes after blocker application, the pH_i of the ouabain- and foliomycin-treated REC was reduced to 6.88 ± 0.09 ($n = 7$) and 6.95 ± 0.08, ($n = 7$), respectively. In the presence of both inhibitors, the pH_i was decreased to 6.79 ± 0.09 ($n = 4$). At the end of the measurement period, we observed a pH_i of 7.04 ± 0.09 and 7.10 ± 0.08 in the presence of ouabain or foliomycin, respectively, and a pH_i of 6.91 ± 0.10 in the presence of both blockers (Fig. 5a).

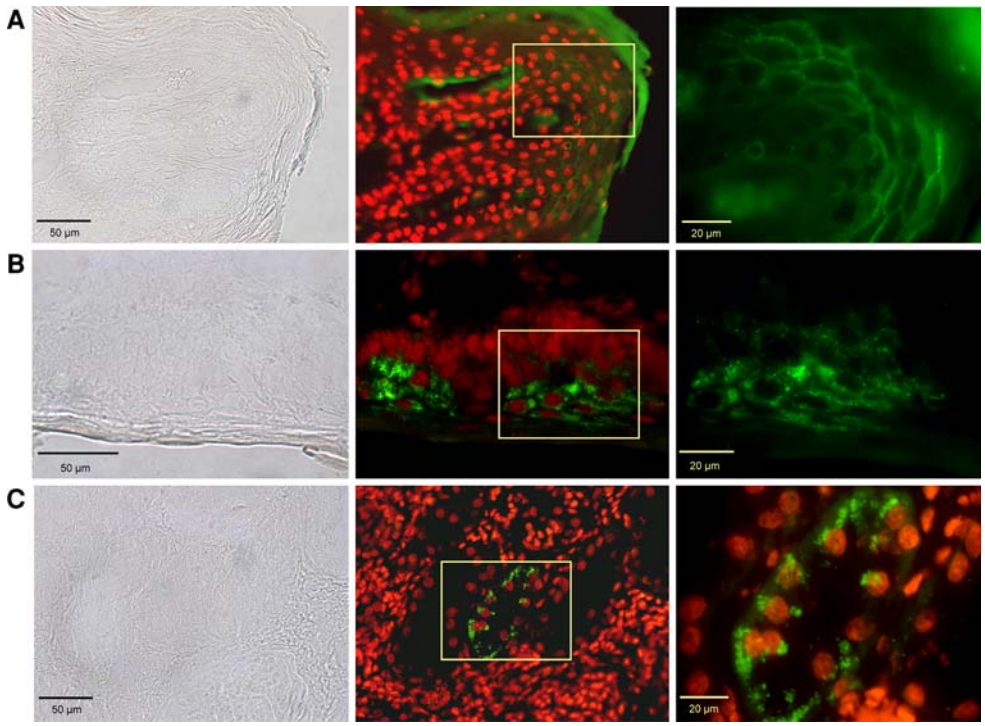

Fig. 4 Immunolocalization of vH^+-ATPase B subunit (*light gray*) in bovine rumen papillae (**a**, **b**) and kidney (**c**) using a polyclonal goat antibody against human vH^+-ATPase B1/2 subunit (**a**) or a monoclonal mouse antibody against yeast vH^+-ATPase 60 kDa-subunit (**b**, **c**) and respective Alexa fluor 488 conjugated secondary antibodies (*left*: transmitted-light micrograph; *middle*: fluorescent image of same area; *right*: higher magnification of *boxed area*). **a** Dominant localization of vH^+-ATPase subunit B in the cytoplasmic membrane of cells in the stratum basale to stratum granulosum. **b** Groups of cells showing dominant cytoplasmic staining. **c** Bovine kidney cortical collecting duct cells showing the typical vH^+-ATPase localization. Cells were co-stained with propidium iodide (*gray*) to label nuclei

We assumed the ouabain-induced pH_i decrease to result from an increased intracellular [Na^+] and thereby reduced Na^+/H^+ exchanger activity. To test this assumption, REC were pre-treated for 10 min with ouabain (0.5 mM), and then exposed for 10 min to amiloride (0.25 mM), a known inhibitor of the Na^+/H^+ exchanger (Schweigel et al. 2005). The sequence of blocker application was changed in other experiments and control measurements were performed without any inhibitor in the extracellular solution. The results of these experiments are summarized in Fig. 5b. The ouabain-induced pH_i decrease (-0.18 ± 0.06 pH units, $n = 3$) was completely abolished after pre-treatment of REC with amiloride ($n = 3$). Moreover, the amiloride-related pH_i reduction amounted to -0.52 ± 0.12 pH units in control REC ($n = 3$) but was reduced to -0.31 ± 0.07 pH units in REC pre-treated with ouabain ($n = 3$).

Discussion

Before the identification of the ruminal vH^+-ATPase (Etschmann et al. 2006), the Na^+/K^+-ATPase was the only active transport mechanism described in rumen epithelium. Therefore, we wished to investigate the expression, localization, and functional activity of both proteins in parallel.

Confirmation of Na^+/K^+-ATPase expression in rumen epithelium

In common with other workers (Graham and Simmons 2005; Hansen 1998; Kristensen et al. 1995), we have confirmed the high expression level and invariable localization of this protein in the cell membrane of REC. As in the only study of the distribution of the Na^+/K^+-ATPase (Graham and Simmons 2005), we have found the protein to be existent in all cells of the stratum basale to stratum granulosum with the highest abundance in basal cells. On the basis of results obtained by the unspecific heavy metal capture technique, Henrikson (1971) has assumed that the activity of the Na^+/K^+-ATPase in ovine rumen epithelium is concentrated in the midepithelial cell layers. However, in the present study we have clearly shown an identical staining pattern in bovine and ovine rumen epithelium. A preponderance of Na^+/K^+-ATPase in the basal cell layers of the epithelium has also been shown for frog skin, another multilayered epithelium (Mills et al. 1977); this ensures the polarity required for transepithelial Na^+ transport. The Na^+ gradient generated by the pump also has a critical role in regulating intracellular Ca^{2+}, Mg^{2+}, and pH_i via Na^+/cation exchange systems (Schweigel et al. 2005, 2006). Disturbance of the Na^+ gradient by application of

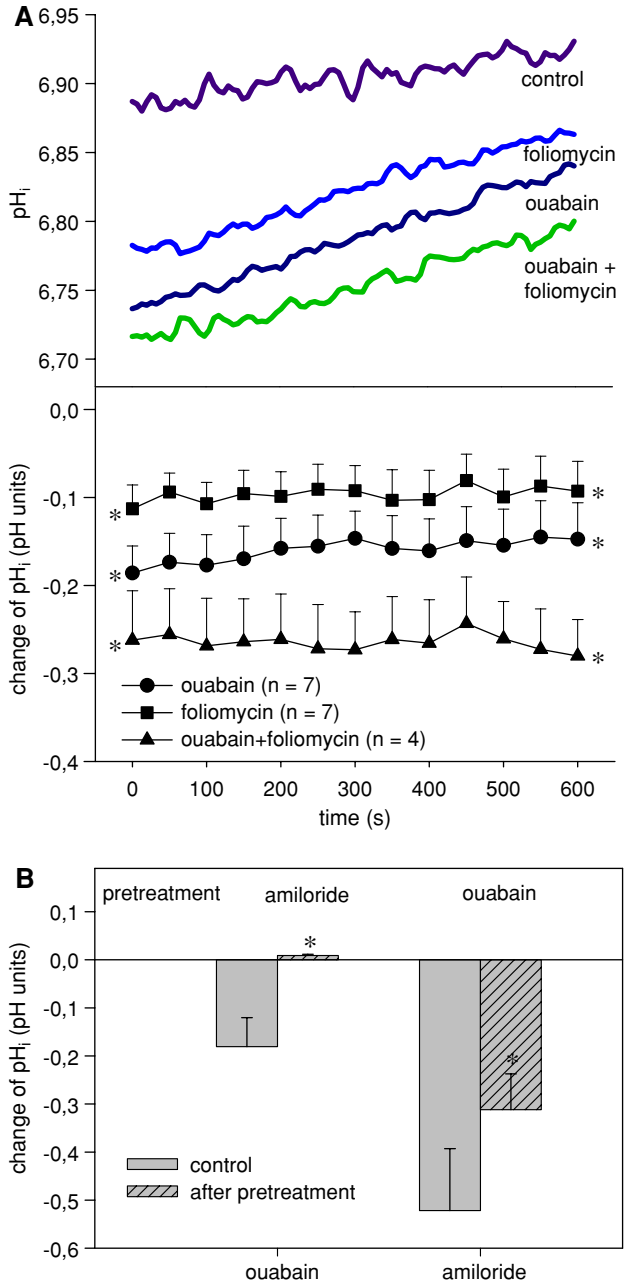

Fig. 5 Effect of vH^+-ATPase and Na^+/K^+-ATPase inhibitors on pH_i of ruminal epithelial cells. Ten-minute measurements were made after a 5-min pre-incubation in either HEPES-buffered NaCl-medium with 20 mM butyrate (control) or the same media with blockers as indicated. **a** The upper part of the figure shows original traces from one experiment. To summarize the inhibitor effects, the mean pH_i reduction from the pH_i measured in control medium without inhibitors has been calculated for the given time points and is shown for each condition. **b** Effect of ouabain or amiloride pre-treatment on pH_i reduction induced by Na^+/H^+ or Na^+/K^+-ATPase inhibition. Blocker concentrations are 2 μM, 0.5 mM and 0.25 mM for foliomycin, ouabain and aniloride, respectively. Values are means ± SE; n = number of single experiments = number of animals. *$P < 0.05$ vs. control

the Na^+/K^+-ATPase inhibitor ouabain, therefore, leads to a significant reduction of pH_i resulting from a decrease in Na^+/H^+ exchanger (NHE) activity. Under HCO_3^- free conditions, the latter has been shown to be the most important pH_i-regulating mechanism in REC (Etschmann et al. 2006; Müller et al. 2000; Schweigel et al. 2000). In HCO_3^- free incubated sheep REC, NHE and vH^+-ATPase activity accounts for about 70 and 30% of H^+ extrusion, respectively, and most (about 50%) of the NHE-mediated component is related to subtype 1 (Etschmann et al. 2006). The relationship between NHE and Na^+/K^+-ATPase has been confirmed by our results showing that inhibition of the NHE by amiloride results in complete abolishment of the ouabain-related pH_i decrease. Moreover, pre-treatment with ouabain reduced the amiloride effect by 40% supporting a decreased NHE activity after inhibition of the Na^+/K^+-ATPase.

Expression of a functional vH^+-ATPase in bovine rumen epithelium

In our previous study (Etschmann et al. 2006), we described, for the first time, the detection of vH^+-ATPase mRNA and protein in sheep rumen epithelial cells. The results from the qPCR and immunoblotting components of this study clearly confirm the expression of a vH^+-ATPase in bovine REC. Using antibodies directed against the vH^+-ATPase B-subunit, we have revealed the existence of this active transport protein in bovine rumen epithelium by immunohistochemistry. Moreover, the functionality of the vH^+-ATPase has been shown by the existence of a foliomycin-sensitive pH_i component in these cells. The pH_i decrease measured after foliomycin application is 0.10 ± 0.03 pH-units, which is in the range (-0.08 to -0.26 pH units) seen for sheep REC (Etschmann et al. 2006) and reported in studies with cells of the human eccrine sweat duct (Granger et al. 2002), cultured rabbit non-pigmented ciliary epithelium (Hou and Delamere 2000) and alveolar macrophages (Heming and Bidani 2002). Thus, the expression of vH^+-ATPase seems to be a generalized property of rumen epithelium.

However, the immunohistochemical results of the present study show vH^+-ATPase B subunit expression in groups of cells only, mainly localized in the stratum spinosum and stratum granulosum of the epithelium. Resulting from a smaller number of vH^+-ATPase-expressing cells, the overall abundance of vH^+-ATPase B subunit is lower than that of Na^+/K^+-ATPase α subunit. This is also reflected by our findings showing that the relative abundance of Na^+/K^+-ATPase α subunit mRNA

and protein is tenfold and 11-fold of those of vH^+-ATPase B subunit, respectively. This indicates that vH^+-ATPase is present in special cells only. In other epithelia, including that of the mammalian kidney collecting duct, urinary bladder, epididymis and vas deferens, amphibian skin and fish gills, vH^+-ATPases are expressed in highly specialized mitochondria-rich (MR) or intercalated cells (Adelsberg and Al-Awqati 1986; Brown and Breton 1996; Ehrenfeld and Klein 1997; Hawkings et al. 2004). Depending on organ function(s), vH^+-localization and co-expression of other transport proteins, MR cells can be divided into subpopulations serving different functions such as elimination of a body acid (α-phenotype) or base (β-phenotype) load, acidification of extracellular compartments, or uptake of Cl^- (γ-phenotype) and nutrients (Brown and Breton 1996; Larsen et al. 1992; Jensen et al. 1997; Dou et al. 2004). The vH^+-ATPase expressing REC have not been characterized yet. Whether, as in renal, amphibian skin and gill epithelia (Bagnis et al. 2001; Ehrenfeld and Klein 1997; Piermarini and Evans 2001), its number and phenotype varies in dependence on extracellular conditions, e.g., $[Na^+]$, remains to be investigated. However, mitochondria are highly abundant in REC (Graham and Simmons 2005) and, in some earlier studies, cytosolic carbonic anhydrase (CA) has been shown to exist in cells from stratum basale to stratum granulosum (Galfi et al. 1982; Asari et al. 1989). Expression of this enzyme is a common feature of MR cells (Bagnis et al. 2001; Brown and Breton 1996; Elbrond et al. 2004), and it is thought that vH^+-ATPase activity mainly depends on protons from CA-mediated hydration of CO_2 (Dou et al. 2004). For the rumen epithelium, the source of CO_2 is not only the metabolic processes of the REC, but also the large CO_2-pool of the ruminal fluid resulting from microbial fermentation of carbohydrates. Therefore, under natural conditions CO_2 could be an important factor for the regulation of ruminal vH^+-ATPase activity and distribution.

In the present study, a variable subcellular distribution of vH^+-ATPase has been observed. Our data demonstrate the appearance of vH^+-ATPase B-subunits in undefined intracellular compartments and also within the plasma membrane of REC or in its close vicinity. Because we used regular fluorescence microscopy in our study, we were not able to discriminate between the two latter possibilities. The vH^+-ATPase is well known as being present in intracellular membrane components such as endosomes, lysosomes, clathrin-coated vesicles, and the Golgi complex (Nanda et al. 1996; Pastor-Soler et al. 2003; Roussa et al. 2001; Sautin et al. 2005). The pump is required for the acidification of vesicles that are involved in the transcytosis of receptor–ligand complexes and other molecules, e.g., NH_3/NH_4^+ (Nelson 1992; Weihrauch et al. 2002). Therefore, the dominant intracellular distribution of REC vH^+-ATPase B-subunit could be indicative of an increased intensity of such processes. The dominant cell-membrane location of ruminal vH^+-ATPase is consistent with its acute regulation in response to physiological stimuli. The recycling of the protein between the plasma membrane and a pool of cytoplasmic vesicles and/or dissociation of V_1 catalytic complex from membrane-bound V_0 domains has been demonstrated in epithelia of kidney, pancreas and placenta (Pastor-Soler et al. 2003; Roussa et al. 2001; Sautin et al. 2005; Skinner et al. 1999; Winter et al. 2004) and in cell types, such as neutrophils, macrophages, and osteoclastes (Lee et al. 1999; Nanda et al. 1996). Regulatory factors in vH^+-ATPase recycling include pH_i, pCO_2, aldosterone, angiotensin II, and glucose (Wagner et al. 1998; Nakamura 2004; Pastor-Soler et al. 2003; Sautin et al. 2005; Winter et al. 2004). We speculate that the preferential expression of vH^+-ATPase in cells of the luminally directed layers of the rumen epithelium in conjunction with a predominant cell-membrane distribution reflects the need of luminal and/or intercellular H^+ for the protonation of SCFA synthesized in the rumen by bacterial fermentation processes (Gäbel et al. 2002). SCFA are the main energetic substrates for ruminants and can be more easily absorbed in their protonated form (Gäbel et al. 2002; Sehested et al. 1999). Recently, Graham et al. (2007) demonstrated a dominant localization of NHE1 at the apical stratum granulosum and proposed that this expression of the protein generates localized extracellular acidity to promote non-ionic, diffusional influx of SCFA into the cytosol of these cells. It can be assumed that a parallel vH^+-ATPase activity in stratum granulosum and spinosum cells can facilitate the diffusional flux of SCFA through the epithelium. Because vH^+-ATPase is Na^+-independent and can work against strong proton gradients, its relevance will increase with high-K^+, low-Na^+ concentrations in the ruminal fluid and in situations with a sudden increase of ruminal fermentation rate, pCO_2 and SCFA concentrations, e.g. after uptake of large, concentrate-rich meals. By extruding H^+ out of REC, vH^+-ATPase may also enhance the intracellular supply of HCO_3^- to a co-expressed HCO_3^-/Cl^- ($SCFA^-$) exchanger (Gäbel et al. 2002; Sehested et al. 1996; Kramer et al. 1996). Thereby, the pump will not only support HCO_3^- secretion into the low-pH ruminal and/or intercellular fluid but also the absorption of Cl^- and of SCFA in their dissociated form. Indirect evidence for the involvement of vH^+-ATPase in ruminal transport processes comes from in vitro and in vivo experiments showing that neither inhibition of the ruminal NHE nor total replacement of luminal Na^+ exerted any significant effect on SCFA absorption (Kramer et al. 1996). In contrast, mucosal nitrate, known to inhibit vH^+-ATPase activity (Gluck et al. 1992), has been demonstrated to

reduce SCFA (propionate) and Cl^- absorption markedly (Kramer et al. 1996; Würmli et al. 1987).

In conclusion, our results clearly show that functional vacuolar-type H^+ pumps are expressed in REC mainly of stratum spinosum and granulosum, and that they are partly localized in the cell membrane. The existence of the vH^+-ATPase as an active transport mechanism in addition to the Na^+/K^+-ATPase implies a special functional role of the protein in the rumen. We suggest that the fast translocation of vH^+-ATPase between cytoplasmic pools and the cell membrane and/or changes in the number of the cells expressing the protein could be important mechanisms to adapt epithelial transport in response to substrate availability.

Acknowledgments We gratefully acknowledge the valuable technical assistance of K. Wolf (Institute of Veterinary Physiology, Free University Berlin) with the Western blots. We also thank R. Brose, H. Pröhl, S. Dwars and K. Marquardt (FBN Dummerstorf) for their excellent technical assistance and Dr. Theresa Jones for linguistic corrections.This study was supported by the DFG (M. Schweigel, SCHW 652).

References

Adelsberg van J, Al-Awqati Q (1986) Regulation o cell pH by Ca^{2+}-mediated exocytotic insertion of H^+-ATPases. J Cell Biol 102:1638–1645

Asari M, Sasaki K, Kano Y, Nishita T (1989) Immunohistochemical localization of carbonic anhydrase isozymes I, II and III in the bovine salivary glands and stomach. Arch Histol Cytol 52:337–344

Bagnis C, Marshansky V, Breton S, Brown D (2001) Remodeling the cellular profile of collecting ducts by chronic carbonic anhydrase inhibition. Am J Physiol Renal Physiol 280:F437–F448

Brown D, Breton S (1996) Mitochondria-rich, proton-secreting epithelial cells. J Exp Biol 199:2345–2358

Brown D, Breton S (2000) H^+V-ATPase dependent luminal acidification in the kidney collecting duct and the epididymis/vas deferens: vesicle recycling and transcytotic pathways. J Exp Biol 203:137–145

Dou H, Xu J, Wang Z, Smith AN, Soleimani M, Karet FE, Greinwald JH, Choo D (2004) Co-expression of pendrin, vacuolar H^+-ATPase α_4-subunit and carbonic anhydrase II in epithelial cells of the murine endolymphatic sac. J Histochem Cytochem 52:1377–1384

Drose S, Bindseil KU, Bowman EJ, Siebers A, Zeeck A, Altendorf K (1993) Inhibitory effect of modified bafilomycins and concanamycins on P- and V-type adenosinetriphosphatases. Biochemistry 32:3902–3906

Ehrenfeld J, Klein U (1997) The key role of the H^+ V-ATPase in acid-base balance and Na^+ transport processes in frog skin. J Exp Biol 200:247–256

Elbrond VS, Jones CJP, Skadhauge E (2004) Localization, morphology and function of the mitochondria-rich cells in relation to transepithelial Na^+-transport in chicken lower intestine (coprodeum). Comp Biochem Physiol A 137:683–696

Etschmann B, Heipertz S, von der Schulenburg A, Schweigel M (2006) A vH^+-ATPase is present in cultured sheep ruminal epithelial cells. Am J Physiol Gastrointest Liver Physiol 291:G1171–G1179

Gäbel G, Aschenbach JR, Müller F (2002) Transfer of energy substrates across the ruminal epithelium: implications and limitations. Anim Health Res Rev 3:15–30

Galfi P, Neogrady S, Kutas F (1980) Culture of ruminal epithelial cells from bovine ruminal mucosa. Vet Res Commun 4:295–300

Galfi P, Kutas F, Neogrady S (1982) Immunohistochemical detection of bovine ruminal carbonic anhydrase isoenzyme. Histochemistry 74:577–584

Gluck SL, Nelson RD, Lee BS, Wang Z, Guo X, Fu J, Zhang K (1992) Biochemistry of the renal V-ATPase. J Exp Biol 172:219–229

Graham C, Simmons NL (2005) Functional organization of bovine rumen epithelium. Am J Physiol Regul Integr Comp Physiol 288:173–181

Graham C, Gatherar I, Haslam I, Glanville M, Simmons NL (2007) Expression and localization of monocarboxylate transporters and sodium/proton exchangers in bovine rumen epithelium. Am J Physiol Regul Integr Comp Physiol 292:997–1007

Granger D, Marsolais M, Burry J, Laprade R (2002) V-type H^+-ATPase in human eccrine sweat duct: immunolocalization and functional demonstration. Am J Physiol Cell Physiol 282:C1454–C1460

Hansen O (1998) Isoform of Na^+,K^+-ATPase from rumen epithelium identified and quantified by immunochemical methods. Acta Physiol Scand 163:201–208

Hawkings GS, Galvez F, Goss GG (2004) Seawater acclimation causes independent alterations in Na^+/K^+- and H^+-ATPase activity in isolated mitochondria-rich cell subtypes of the rainbow trout gill. J Exp Biol 207:905–912

Heming TA, Bidani A (2002) Plasmalemmal H^+ extruders in mammalian alveolar macrophages. Comp Biochem Physiol A 133:143–150

Henrikson RC (1971) Mechanism of sodium transport across ruminal epithelium: a study by electron microscopy using horseradish peroxidase, lanthanum and ferritin. J Ultrastruct Res 34:72–82

Hou Y, Delamere NA (2000) Studies on H^+-ATPase in cultured rabbit nonpigmented ciliary epithelium. J Membr Biol 173:67–72

Jensen LJ, Sorensen JN, Larsen EH, Willumsen NJ (1997) Proton activity of mitochondria-rich cells. The interpretation of external proton-concentration gradients. J Gen Physiol 109:73–91

Karwatowska-Prokopczuk E, Nordberg JA, Li HL, Engler RL, Gottlieb RA (1998) Effect of vacuolar proton ATPase on pH_i, Ca^{2+} and apoptosis in neonatal cardiomyocytes during metabolic inhibition/recovery. Circ Res 82:1139–1144

Kelly JM, McBride BW, Milligan LP (1993) In vitro ouabain-sensitive respiration and protein synthesis in ruminal epithelial papillae of Hereford steers fed either alfalfa or bromegrass hay once daily. J Anim Sci 71:2799–2808

Kramer T, Michelberger T, Gürtler H, Gäbel G (1996) Absorption of short-chain fatty acids across rumen epithelium of sheep. J Comp Physiol B 166:262–269

Kristensen NB, Hansen O, Clausen T (1995) Measurement of the total concentration of functional Na^+, K^+-pumps in the rumen epithelium. Acta Physiol Scand 155:67–76

Larsen EH, Willumsen NJ, Christoffersen BC (1992) Role of proton pump of mitochondria-rich cells for active transport of chloride ions in toad skin epithelium. J Physiol (Lond) 450:203–216

Lee BS, Gluck SL, Holliday LS (1999) Interaction between vacuolar H^+-ATPase and microfilaments during osteoclast activation. J Biol Chem 41:29164–29171

Löhrke B, Viergutz T, Krüger B (2005) Polar phospholipids from bovine endogenously oxidized low density lipoprotein interfere with follicular thecal function. J Mol Endocrinol 35:531–545

Mills JW, Ernst SA, DiBona DR (1977) Localization of Na-pump sites in frog skin. J Cell Biol 73:88–110

Müller M, Aschenbach JR, Gäbel G (2000) Role of Na^+/H^+ exchange and HCO_3^- transport in pH_i recovery from intracellular acid load in cultured epithelial cells of sheep rumen. J Comp Physiol B 170:337–343

Nakamura S (2004) Glucose activates H^+-ATPase in kidney epithelial cells. Am J Physiol Cell Physiol 287:C97–C105

Nanda A, Brumell JH, Nordström T, Kjeldsen L, Sengelav H, Borregaard N, Rotstein OD, Grinstein S (1996) Activation of proton pumping in human neutrophils occurs by exocytosis of vesicles bearing vacuolar-type H^+-ATPases. J Biol Chem 271:15963–15970

Nelson N (1992) Structure and function of V-ATPases in endocytotic and secretory organelles. J Exp Biol 172:149–153

Pastor-Soler N, Beaulieu V, Litvin TN, Da Silva N, Chen Y, Brown D, Buck J, Levin LR, Breton S (2003) Bicarbonate-regulated adenyl cyclase (sAC) is a sensor that regulates pH-dependent v-ATPase recycling. J Biol Chem 278:49523–49529

Piermarini PM, Evans DH (2001) Immunochemical analysis of the vacuolar proton-ATPase B-subunit in the gills of a euryhaline stingray (*Dasyatis sabina*): effects of salinity and relation to Na^+/K^+-ATPase. J Exp Biol 204:3251–3259

Roussa E, Alper SL, Thevenod F (2001) Immunolocalization of anion exchanger AE2, Na^+/H^+ exchangers NHE1 and NHE4, and vacuolar type H^+-ATPase in rat pancreas. J Histochem Cytochem 49:463–474

Rozengurt E (1980) Stimulation of Na influx, Na–K pump activity and DNA synthesis in quiescent cultured cells. Adv Enzyme Regul 19: 61–85

Sautin YY, Lu M, Gaugler A, Zhang L, Gluck SL (2005) Phosphatidylinositol 3-kinase-mediated effects of glucose on vacuolar H^+-ATPase assembly, translocation, and acidification of intracellular compartments in renal epithelial cells. Mol Cell Biol 25:575–589

Schweigel M, Martens H (2003) Anion-dependent Mg^{2+} influx and a role for a vacuolar H^+-ATPase in sheep ruminal epithelial cells. Am J Physiol Gastrointest Liver Physiol 285:G45–G53

Schweigel M, Vormann J, Martens H (2000) Mechanisms of Mg^{2+} transport in cultured ruminal epithelial cells. Am J Physiol Gastrointest Liver Physiol 278:G400–G408

Schweigel M, Freyer M, Leclercq S, Etschmann B, Lodemann U, Böttcher A, Martens H (2005) Luminal hyperosmolarity decreases Na transport and impairs barrier function of sheep rumen epithelium. J Comp Physiol B 175:575–591

Schweigel M, Park H-S, Etschmann B, Martens H (2006) Characterization of the Na^+-dependent Mg^{2+} transport in sheep ruminal epithelial cells. Am J Physiol Gastrointest Liver Physiol 290:G56–G65

Sehested J, Diernaes L, Moller PD, Skadhauge E (1996) Transport of sodium across the isolated rumen epithelium: interaction with short-chain fatty acids, chloride and bicarbonate. Exp Physiol 81:79–94

Sehested J, Diernaes L, Moller PD, Skadhauge E, Sehested J, Diernaes L, Moller PD, Skadhauge E (1999) Ruminal transport and metabolism of short chain fatty acids (SCFA) in vitro: effects of SCFA chain length and pH. Comp Biochem Physiol A 123:359–368

Sennoune SR, Bakunts K, Martinez GM, Chua-Tuan JL, Kebir Y, Attaya MN, Martinez-Zaguilan R (2004) Vacuolar H^+-ATPase in human breast cancer cells with distinct metastatic potential: distribution and functional activity. Am J Physiol Cell Physiol 286:C1443–C1452

Skinner MA, MacLaren LA, Wildeman AG (1999) Stage-dependent redistribution of v-ATPase during bovine implantation. J Histochem Cytochem 47:1247–1254

Standley PR, Zhang F, Zayas RM, Muniyappa R, Walsh F, Cragoe E, Sowers JR (1997) IGF-1 regulation of Na^+–K^+-ATPase in rat arterial smooth muscle. Am J Physiol Endocrinol Metab 273:E113–E121

Ulbrich SE, Rehfeld S, Bauersachs S, Wolf E, Rottmayer R, Hiendleder S, vermehren M, Sinowatz F, Meyer HHD (2006) Region-specific expression of nitric oxide synthases in the bovine oviduct during the oestrous cycle and in vitro. J Endocrinol 188:205–213

Wagner CA, Giebisch G, Lang F, Geibel JP (1998) Angiotensin II stimulates vesicular H^+-ATPase in rat proximal tubular cells. PNAS 95:9665–9668

Weihrauch D, Ziegler A, Siebers D, Towle DW (2002) Active ammonia secretion across the gills of the green shore crab *Carcinus maenas*: participation of Na^+/K^+-ATPase, V-type H^+-ATPase and functional microtubules. J Exp Biol 205:2765–2775

Winter C, Schulz N, Giebisch G, Geibel JP, Wagner CA (2004) Nongenomic stimulation of vacuolar H^+-ATPases in intercalated renal tubule cells by aldosterone. PNAS 101:2636–2641

Würmli R, Wolffram S, Scharrer E (1987) Inhibition of chloride absorption from sheep rumen by nitrate. J Vet Med A 34:476–479

Zouzoulas A, Dunham PB, Blostein R (2005) The effect of the gamma modulator on Na/K pump activity in intact mammalian cells. J Membr Biol 204:49–56